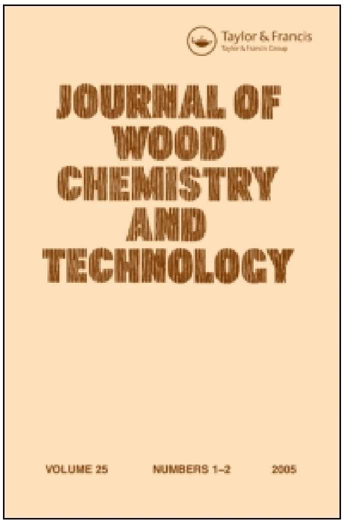

Journal of Wood Chemistry and Technology
Publication details, including instructions for authors and subscription information:
http://www.informaworld.com/smpp/title~content=t713597282

Chlorate Formation in Chlorine Dioxide Delignification—An Analysis via Elementary Kinetic Modeling

Ville Tarvo[a]; Tuula Lehtimaa[b]; Susanna Kuitunen[a]; Ville Alopaeus[a]; Tapani Vuorinen[b]
[a] Department of Biotechnology and Chemical Technology, Helsinki University of Technology (TKK), Helsinki, Finland [b] Department of Forest Products Technology, Helsinki University of Technology (TKK), Helsinki, Finland

To cite this Article Tarvo, Ville , Lehtimaa, Tuula , Kuitunen, Susanna , Alopaeus, Ville and Vuorinen, Tapani(2009) 'Chlorate Formation in Chlorine Dioxide Delignification—An Analysis via Elementary Kinetic Modeling', Journal of Wood Chemistry and Technology, 29: 3, 191 — 213

To link to this Article: DOI: 10.1080/02773810802650351

URL: http://dx.doi.org/10.1080/02773810802650351

Journal of Wood Chemistry and Technology, 29: 191–213, 2009
Copyright © Taylor & Francis Group, LLC
ISSN: 0277-3813 print / 1532-2319 online
DOI: 10.1080/02773810802650351

Taylor & Francis
Taylor & Francis Group

Chlorate Formation in Chlorine Dioxide Delignification—An Analysis via Elementary Kinetic Modeling

Ville Tarvo,[1] Tuula Lehtimaa,[2] Susanna Kuitunen,[1]
Ville Alopaeus,[1] and Tapani Vuorinen[2]
[1]Department of Biotechnology and Chemical Technology, Helsinki University of Technology (TKK), Helsinki, Finland
[2]Department of Forest Products Technology, Helsinki University of Technology (TKK), Helsinki, Finland

Abstract: Elementary kinetic modeling was used to study the mechanism of chlorate formation in chlorine dioxide delignification. Reaction conditions reflecting typical industrial processes ($T = 50°C$, pH 1.5–4) were examined. Fe mediated Cl(III) decomposition and a reaction between hypochlorous acid and chlorous acid (or their equilibrium counterparts) were found to be the major reaction routes responsible for chlorate formation at pH < 3. The latter route accounts for chlorate formation at pH $\geq$ 3. The rate of chlorous acid ($HClO_2$) self-decomposition was too slow either to compete against the other routes (pH < 3) or to yield notable amounts of chlorate within the given time frame (pH $\geq$ 3). The results suggest that chlorate formation could be suppressed, without adverse effects on chlorine dioxide regeneration, by aiming for end pH 3–3.5, ensuring a moderate chloride ion concentration and by favoring concentrated solutions/suspensions.

Keywords: Bleaching, chlorate, chlorine dioxide, chlorite, delignification, inorganic reactions, modeling, predictive modeling, reaction kinetics

Gratitude is shown for all parties in the Advanced Bleaching Plant project: the researchers for input in model development; the Technology Development Agency of Finland (TEKES); and participating companies for financial support. The Graduate School in Chemical Engineering is acknowledged for funding. Deep gratitude is shown for Professor Gérard Mortha for enlightened discussions. Professor Istvan Fabian is thanked for providing the very valuable Fe mediated Cl(III) decomposition measurement results.

Address correspondence to Ville Tarvo, Department of Biotechnology and Chemical Technology, P.O. Box 6100, Helsinki University of Technology (TKK), Helsinki FI-02015, Finland. E-mail: ville.tarvo@tkk.fi

INTRODUCTION

Chlorite ion (ClO_2^-) and hypochlorous acid (HOCl) are the primary reduction products of chlorine dioxide (ClO_2) in ClO_2 delignification of chemical pulp.[1–5] Both compounds react further in numerous reactions and yield various oxy- and organo-chlorine species as well as chloride ion (Cl^-) as the stable final products.[4] Chlorate ion (ClO_3^-) is one of the formed oxy-chlorine species. It is also suggested to be formed directly from chlorine dioxide.[4,6] Chlorate formation is considered wasteful, as the compound possesses a high apparent oxidation power (valence V^+) but it is unable to facilitate delignification reactions.[7,8] Chlorate is also highly toxic (acute toxicity <0.1 mg/l) to certain macro brown algal species.[9,10] Several reports deal with various aspects of chlorate formation in delignification and bleaching.[8,9,11–19] A traditional way to examine the formation mechanism is to record chlorate yield under various conditions and use the reaction variable dependencies to analyze and exclude the reaction alternatives. Other methods comprise trapping of intermediately formed hypochlorous acid[16,20] and utilization of model compounds.[11,21] These studies suggest that chlorate is produced at least through chlorous acid self-decomposition (1),[4,8,19] in a reaction between chlorous acid and hypochlorous acid (2),[16,17] and by free radical addition to chlorine dioxide (3).[4,6,19] Reactions (2–3) are overall reactions depicting the reactants and stable final products, but disregard any intermediate steps or species. Alkaline decomposition of chlorine dioxide (4) is frequently brought up as another origin for chlorate.[12,14,15,17,18,22] The decomposition rate is, however, slow already in mildly acidic solutions.[18,23,24] Thus, delignifying reactions are expected to consume chlorine dioxide much faster than alkaline decomposition in acidic medium.[15,18] Alkaline decomposition of chlorine dioxide is not considered further in this work.

$$2\,HClO_2 \rightarrow HOCl + ClO_3^- + H^+ \qquad (1)$$

$$a\,HClO_2 + HOCl \rightarrow b\,ClO_3^- + c\,ClO_2\cdot + d\,Cl^- + e\,H^+ + f\,H_2O$$
(2—unbalanced overall reaction)

$$ClO_2\cdot + \text{free radical} + H_2O \rightarrow ClO_3^- \qquad \text{(3—unbalanced overall reaction)}$$

$$2\,ClO_2\cdot + OH^- \rightarrow ClO_2^- + ClO_3^- + H^+ \qquad \text{(4—overall reaction)}$$

The traditional way of examining chlorate formation suffers from the fact that the relative importance of numerous reactions is evaluated only at a qualitative level. The importance of chlorous acid disproportionation (1) is claimed to increase with acidity. This is a qualitative implication from the reaction rate equation. It has, however, not been examined whether the reaction possesses kinetic prerequisites to contribute to chlorate formation even at the lowest pH levels encountered in delignification applications (around pH 2). Delignification and bleaching experiments have produced rather controversial results concerning the pH dependency of chlorate formation: chlorate production has been shown to increase,[12,16] decrease,[8,9,13,15,17,19] or to fluctuate with pH.[25] The most extensive effort to explain the pH dependency is based on the Taube-Dodgen (TD) mechanism, which covers the intermediate steps and species of overall reaction (2).[16,26] The original TD mechanism, postulated in the 1940s, has been cultivated in several subsequent studies[27–31] and the prediction of the most recent mechanism should be examined.

This work aims at clarifying the mechanistic aspects of chlorate formation in chlorine dioxide delignification. The analysis is done using elementary reaction kinetic modeling and the latest mechanistic descriptions. Kinetic information mainly from the literature, partly determined in this work, is gathered in a model and used to study the reaction rates and overall stoichiometries under typical delignification conditions. The used modeling approach provides a straightforward method for examining both individual reactions as well as systems consisting of competing and consecutive reactions. The reaction routes are first examined one at a time (excluding all other reactions). The routes are then made to compete with each other in order to predict the total amount and pH dependency of chlorate formation. Elementary kinetic modeling, although rarely utilized in studies related to pulp and paper industry, is commonly used in the field of petrochemistry, combustion technology, and chemical reaction engineering.

THEORETICAL BACKGROUND AND SIMULATION MODEL

All simulations were performed with Flowbat software.[32] The initial solution composition and conditions were first defined. The solution composition development, that is, the progress of reactions, was evaluated through reaction rate equations. Reaction rate equations produce time derivatives for reactant and product concentrations. As an example, the equations given in (e1), where brackets indicate component concentrations, may be written for chlorous acid self-decomposition reaction 1. Analogous equations were written for all reactions under investigation. The obtained group of initial value ordinary differential equations was solved with an ordinary differential equation solver. All reactions without specific catalysis were assumed to obey elementary kinetics, that is, the rates were first order with respect to each reacting compound, and the reaction rates were proportional only to the concentrations of the reacting species and the reaction rate coefficient (k_r). Any overall reactions (except for auxiliary reactions involving organic compounds) were broken up into elementary steps according to the applied mechanistic schemes. Thus, any rate or stoichiometry dependencies related to reaction conditions or solution composition were inherently incorporated in the model. The temperature dependency of the reaction rate coefficients was modeled with the Arrhenius equation (e2), where A_r and $E_{a,r}$ are the reaction specific frequency factor and activation energy, respectively, R is the molar gas constant, and T is temperature in Kelvins.

The concept of elementary kinetic modeling assumes that the provided rate parameters and models are universal. They are applicable in any reaction system so long as all participating reactions are incorporated. Thus, rate parameters and equations may be collected from studies applying simpler systems and combined to investigate a more complex problem, as is done in this study. The validity of the kinetic descriptions in the simpler systems (comparison of model predictions against experimental results) is demonstrated in the original reports. The applied chlorate formation reaction schemes and rate parameters are introduced below. Reactions assumed to contribute to chlorite consumption or affect the chlorate forming reactions in delignification environment are considered in the "Total Chlorate Formation" section.

$$-\frac{d[HClO_2]}{dt} = 2\cdot\frac{d[HOCl]}{dt} = 2\cdot\frac{d[ClO_3^-]}{dt} = 2\cdot\frac{d[H^+]}{dt} = k_1\cdot[HClO_2]^2 \tag{e1}$$

$$k_r = A_r\cdot\exp(-E_{a,r}/RT) \tag{e2}$$

Chlorous Acid Self-Decomposition

The kinetics and stoichiometry of chlorous acid self-decomposition is discussed in several reports.[26,27,29,31,33,34] Lehtimaa et al.[35] have recently clarified the scheme with experiments and kinetic analysis at pH 1–3 in absence of transition-metal ions. The reaction occurs over a single step (1) and has a rate coefficient $k_1 = 0.0021\ M^{-1}s^{-1}$ at 25°C and activation energy $E_{a,1} = 84$ kJ/mol. The reaction is occasionally proposed to yield chlorine dioxide and chloride ions.[4,16] In such cases the subsequent reactions of the produced hypochlorous acid are combined in the stoichiometry. In this study the reaction between hypochlorous acid and chlorous acid is considered as a separate reaction route (see the following section), because in delignification environment hypochlorous acid may be produced and consumed through several processes.

Chlorous acid is in equilibrium with chlorite ion via reaction (5). Together they are referred to as Cl(III), according to the oxidation state of chlorine. The degree of Cl(III) protonation changes with pH. This was taken into account via dissociation coefficient $K_{a,5}$ (the kinetics of the protolysis reaction is extremely rapid and was thus considered irrelevant in this work). The value of $K_{a,5}$ at a desired temperature was computed from thermodynamic constants with

Table 1. The effect of temperature on chlorous acid dissociation coefficient

T/°C	20	40	50	60	70
$K_{a,5}$/ M	0.011	0.0078	0.0065	0.0056	0.0048
$pK_{a,5}$	1.96	2.11	2.19	2.25	2.32

equations (e3) and (e4). The enthalpy of formation (ΔH_f°) and entropy (S°) values were obtained from literature.[36] The temperature variance of $K_{a,5}$ is demonstrated in Table 1. The reaction scheme used in chlorous acid self-decomposition simulations included reactions (1), (5) and the autoprotolysis of water. The temperature dependency of water auto-protolysis was incorporated in a similar manner as for reaction (5).

$$HClO_2 \leftrightarrows ClO_2^- + H^+ \tag{5}$$

$$K = \exp[-\Delta G_{freaction}/(R \cdot T)] \tag{e3}$$

$$\Delta G_{freaction} = \Sigma_p\{\Delta H_{f,p} - S_p \cdot T\} - \Sigma_r\{\Delta H_{f,r} - S_r \cdot T\} \tag{e4}$$

where p = products and r = reactants.

The Reaction Between Chlorous Acid/Chlorite and Hypochlorous Acid/Chlorine

The overall reaction (2) proceeds via several elementary steps. Hypochlorous acid reacts rapidly with chlorous acid in reaction (6).[30,34,37] The first step produces an extremely rapidly reacting species, Cl_2O_2, which has not been isolated in a solution state.[29,30] A recently proposed mechanism for Cl_2O_2 consumption contains three parallel paths (8–10), from which the first two exhibit a chloride ion catalysis.[29] In the pioneering mechanism of Taube and Dodgen[26] chlorine dioxide was formed in a bimolecular Cl_2O_2 reaction. This proposition was based on findings that ClO_2 is the predominant product in concentrated Cl(III) solutions. Concentrated Cl(III) solutions lead to rapid Cl_2O_2 formation, and a second order process with regards to Cl_2O_2 would explain the observed effect. Reaction (9), however, also explains the concentration dependence and it has a more solid theoretical basis.[30] The replacement of the second order process with reaction (9) was first proposed by Hong and Rapson[27] and it has received acceptance in numerous subsequent studies.[18,28–31] The scheme used in this study (8–10) is based on the Hong-Rapson-mechanism. If chloride ions are present, hypochlorous acid forms an equilibrium pair with elemental chlorine (11_{for}, 11_{rev}).[38] Chloride ion is the main reduction product of chlorine dioxide in bleaching applications,[8,19,39] and thus its presence is expected. A reaction between chlorine and chlorite (7) serves as an additional source for Cl_2O_2.[30,34,37] Reactions (6) and (7) are significantly slower than the subsequent Cl_2O_2 consuming reactions (8–10). Therefore, reactions (6) and (7) define the overall reaction rate and reactions (8–10) dictate the observed stoichiometry. The reaction condition dependent overall stoichiometry is given by reaction (2).

The overall reaction produces substantial amounts of chlorine dioxide (through reaction step 9). In delignification environment the generated chlorine dioxide reacts rapidly with organic substrates. In order to get the full yield of chlorate, as opposed to just a once-through yield, reaction (12) is introduced. Reaction (12) represents oxidation of lignin or any other organic substrate (indicated with pseudo-component Org,) by chlorine dioxide. The regenerated chlorine dioxide is assumed to produce chlorite and hypochlorous acid in a similar manner as “fresh” chlorine dioxide (discussed in detail in the section “Initial Conditions”). The chlorite:hypochlorous acid ratio in reaction (12) is set to 1:1 for simplicity (the ratio in which chlorite and hypochlorous acid are formed from chlorine dioxide is discussed later in more detail). The organic pseudo-component, Org, was assumed to be available in excess ($[\mathrm{Org}]_0 = 0.01$ M). The reaction rate is first order with respect to ClO_2 and Org.

Rate-Determining Step

$$\mathrm{HClO_2 + HOCl \rightarrow Cl_2O_2 + H_2O} \tag{6}$$

$$\mathrm{ClO_2^- + Cl_2 \rightarrow Cl_2O_2 + Cl^-} \tag{7}$$

Stoichiometry-Determining Step

$$\mathrm{Cl_2O_2 + H_2O \rightarrow ClO_3^- + Cl^- + 2\,H^+} \tag{8}$$

$$\mathrm{Cl_2O_2 + ClO_2^- \rightarrow 2\,ClO_2\cdot + Cl^-} \tag{9}$$

$$\mathrm{Cl_2O_2 + ClO_2^- + H_2O \rightarrow 2HOCl + ClO_3^-} \tag{10}$$

$$\mathrm{HOCl + H^+ + Cl^- \leftrightarrows Cl_2 + H_2O} \qquad (11_{\mathrm{for}},\ 11_{\mathrm{rev}})$$

$$\mathrm{2ClO_2\cdot + Org + H_2O \rightarrow HOCl + ClO_2^- + H^+ + Org_{ox}}$$
(12—apparent overall reaction)

The kinetic parameters for reactions (6–11) are given in Table 2. Activation energy was available only for reactions (7) and (11_{for}, 11_{rev}). The activation energies of the other reactions were set to the same value (39.9 kJ/mol) as reported

Table 2. Rate parameters for the reaction system involving chlorous acid and hypochlorous acid

Reaction	Rate coefficient, k, at 25°C	E_a/kJ·mol^{-1}	Ref
6	$k_6 = 2.1 \cdot 10^4\ M^{-1}s^{-1}$	[b]39.9	[30]
7	$k_7 = 1.6 \cdot 10^4\ M^{-1}s^{-1}$	39.9	[37]
8	$k_8 = 1 \cdot 10^3\ s^{-1}$	[b]39.9	[29]
	[a]$k'_8/k_8 = 2.85 \cdot 10^2 M^{-1}$		
9	$k_9/k_8 = 2.01 \cdot 10^4\ M^{-1}$	[b]39.9	[29]
	[a]$k'_9/k_9 = 4.2 \cdot 10^2\ M^{-1}$		
10	$k_{10} / k_8 = 1.11 \cdot 10^4\ M^{-1}$	[b]39.9	[29]
$11_{,for}$	$k_{11,for} = 1.1 \cdot 10^4\ M^{-2}s^{-1}$	[c]31	
$11_{,rev}$	$k_{11,rev} = 22\ s^{-1}$	[c]62	[40]

[a] Rate coefficient for the chloride ion catalyzed route.

[b] Assumed.

[c] The E_a-values and ionic strength dependence was adopted from experimental results reported by Wang and Margerum.[40]

Rev = reverse reaction, for = forward reaction.

for reaction (7). This keeps the relative rates of reactions (6–10) at the ratio reported at 25°C, irrespective of the temperature. Using a constant rate ratio valid at least at one temperature was considered a better assumption than applying arbitrary activation energies. The concentration of Cl(III) is generally higher than that of chlorine dioxide for the bulk of the delignification time.[4,39] The very first moments of the process, when chlorine dioxide is rapidly consumed and Cl(III) accumulates, is an exception.[39] The rate coefficient k_{12} was set to $k_{12} = 2 \cdot 10^5\ M^{-1}s^{-1}$ (T = 50°C) in order to maintain the concentration of ClO_2 below Cl(III) in all simulations. The reaction scheme used in the simulations included reactions (5–12) and the autoprotolysis of water.

Chlorate Formation Through Radical Chemistry

Some studies suggest that chlorate formation via chlorine dioxide coupling with Cl and ClO radicals could be notable (3).[11,21] This coupling reaction is also considered to provide a radical scavenging mechanism observed in chlorine dioxide bleaching.[6,41] Several studies that have been conducted in much simpler reaction systems, however, indicate that chlorine radicals react rapidly with Cl(III) and produce chlorine dioxide as a stable final product.[28,42,43] Thus, the postulation of direct radical coupling via chlorine dioxide sounds highly unlikely. It is more probable that the observed radical scavenging properties relate to Cl(III) arising as a reduction product from ClO_2. Hence, the focus is hereafter shifted on the interaction of chlorine radicals with Cl(III).

Fe Mediated Cl(III) Decomposition

In acidic solutions ferric ion (Fe^{3+}) reacts with chlorite ion to give chlorine dioxide and ferrous ion (Fe^{2+}) (13).[28,44] Ferrous ion reacts further with chlorite and chlorous acid to form chlorine radicals (e.g., Cl or ClO) (14 and 15).[42,43,45] The produced chlorine radicals lead to chlorate production via Cl(III) decomposition (16). Two models describing the Fe mediated radical formation and the associated Cl(III) decomposition are available.[28,43] Both models are based on experiments where hypochlorous acid has not been trapped. Thus, the proposed mechanisms are strongly influenced by the assumption of how hypochlorous acid reacts further with Cl(III). Fabian and Gordon[28] used a HOCl reaction scheme with anomalous rate parameters: Cl_2O_2 consumption was assumed to occur through reactions (8) and (9) only; the applied rate coefficient ratio was $k_9/k_8 = 50\ M^{-1}$. Other reports postulate k_9/k_8 ratios above $10^4\ M^{-1}$.[29,30] Schmitz and Rooze[43] verified their model only qualitatively and left several rate parameters unspecified (k_9/k_8 among others). Neither of the models can therefore be accepted directly. In order to obtain a suitable model, the previously unknown rate parameters in the Schmitz and Rooze model were determined. Reactions (6–11, Table 2) were used in the regression procedure to model the behavior of hypochlorous acid. Reactions (1) and (5) were also included. The regression was made against the experimental results of Fabian and Gordon.[28] The parameter optimization was done with KinFit software[46] where a nonlinear simultaneous curve fitting technique[47] applying Levenberg-Marquardt method (uniform weighting) was used.[48] The determined rate parameter values are shown in Table 3. Predictions given by our model and by the model of Fabian and Gordon are compared against experimental results in Figures 1 and

Table 3. Rate parameters for Fe mediated Cl(III) decomposition reactions

Reaction	Rate coefficient, k, at 25°C	E_a / kJ·mol^{-1}	Ref
13	$k_{13} = 269\ M^{-1}s^{-1}$	95	[43]
	$k_{13,rev} = 4.7 \cdot 10^5\ M^{-1}s^{-1}$	^{a}95	^{b}
14	$k_{14} = 930\ M^{-1}s^{-1}$	^{a}95	[43]
15	$k_{15} = 530\ M^{-1}s^{-1}$	^{a}95	^{b}
16/19	$k_{16}/k_{19} = 2.2 \cdot 10^{-4}$	—	^{b}
17/18	k_{17}/k_{18} = very small	—	^{b}
	Equilibrium constant, K, at 25°C		
20	$K_{20} = 6.5 \cdot 10^{-3}\ M^1$	^{c}	[36]
21	$K_{21} = 4.9 \cdot 10^{-7}\ M^1$	^{c}	[36]
22	$K_{22} = 1.6 \cdot 10^{-39}\ M^4$	^{c}	[36]

[a] Assumed.
[b] Determined in this work.
[c] Temperature dependence computed via thermodynamic constants.
Rev = reverse reaction, for = forward reaction.

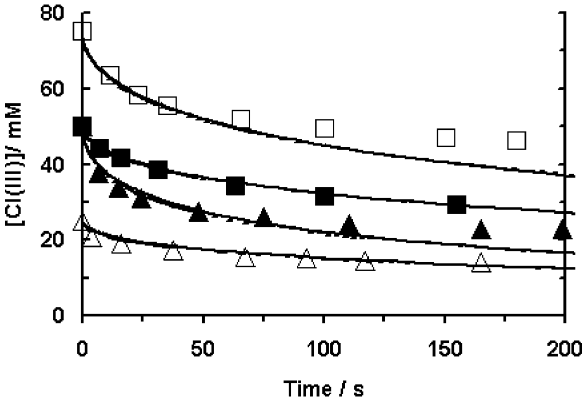

Figure 1. Fe mediated Cl(III) decomposition: *bullets*—experimental, *solid line*—the model of this article, *dashed line*—the model of Fabian and Gordon. Experimental data is provided by Fabian and Gordon.[28] (□)—$[Cl(III)]_0 = 7.50 \cdot 10^{-2}$ M, $[Fe^{3+}] = 1.39 \cdot 10^{-3}$ M, pH = 1.75; (■)—$[Cl(III)]_0 = 4.99 \cdot 10^{-2}$ M, $[Fe^{3+}] = 1.39 \cdot 10^{-3}$ M, pH = 1.25; (▲)—$[Cl(III)]_0 = 5.00 \cdot 10^{-2}$ M, $[Fe^{3+}] = 4.20 \cdot 10^{-3}$ M, pH = 1.75; (Δ)—$[Cl(III)]_0 = 2.5 \cdot 10^{-2}$ M, $[Fe^{3+}] = 1.39 \cdot 10^{-3}$ M, pH = 1.75.

2. Our model yields a very similar prediction as that of Fabian and Gordon. The curves from the two models coincide in Figure 1. Our model gives a slightly better prediction for chlorine dioxide formation at high Cl(III) concentration (Figure 2). The experimental reaction rate appears to level off more strongly than is estimated (Figures 1 and 2). This may result from a slow formation of an unknown inactive Fe-species. Solving the incoherence would, however, require more experiments and is outside of the scope of this study. The Cl and ClO radicals are very reactive and only the ratio of their parallel reaction rates could be determined (17/18 and 16/19). The very small ratio k_{17}/k_{18} implies that Cl radicals are consumed by Fe^{2+} exclusively, and reaction (17) is insignificant.

Additional Sources for Cl and ClO Radicals

Model compound studies indicate that ClO radicals are produced also through two-electron reduction of chlorine dioxide by olefinic structures.[11,21] Due to a lack of suitable experimental information to quantify these reactions they are excluded from the model. Radical generation through chlorine or hypochlorous acid is considered unimportant due to very low concentrations of Cl_2 and HOCl in delignification.

In delignification environment the chlorine dioxide produced in reaction (13) would be rapidly consumed by organic substrates. Hence, reaction (12) is again included in the simulations (detailed reasoning and the rate parameter are

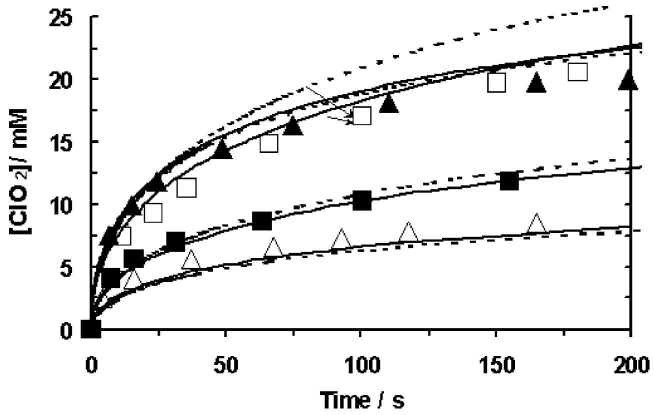

Figure 2. ClO_2 formation from Fe mediated Cl(III) decomposition: *bullets*—experimental, *solid line*—the model of this article, *dashed line*—the model of Fabian and Gordon. Experimental data is provided by Fabian and Gordon.[28] (□)— $[Cl(III)]_0 = 7.50 \cdot 10^{-2}$ M, $[Fe^{3+}] = 1.39 \cdot 10^{-3}$ M, pH = 1.75; (■)—$[Cl(III)]_0 = 4.99 \cdot 10^{-2}$ M, $[Fe^{3+}] = 1.39 \cdot 10^{-3}$ M, pH = 1.25; (▲)—$[Cl(III)]_0 = 5.00 \cdot 10^{-2}$ M, $[Fe^{3+}] = 4.20 \cdot 10^{-3}$ M, pH = 1.75; (Δ)—$[Cl(III)]_0 = 2.5 \cdot 10^{-2}$ M, $[Fe^{3+}] = 1.39 \cdot 10^{-3}$ M, pH = 1.75.

given in the previous section). The experimental data used in regression was obtained at a single temperature (25°C). Thus the activation energy of reactions (13_{rev}), (14), and (15) could not be determined. The activation energies of these reactions were set to the same value as reported for reaction (13_{for}). This keeps the relative rates of reactions (13–15) at the ratio determined at 25°C, irrespective of the temperature. Using a constant rate ratio valid at least at one temperature was considered a better assumption than applying arbitrary activation energies. The reaction scheme used for Fe mediated Cl(III) decomposition simulations included reactions (5), (12–22), and the autoprotolysis of water.

$$ClO_2^- + Fe^{3+} \leftrightarrows ClO_2 + Fe^{2+} \qquad (13_{for}, 13_{rev})$$

$$HClO_2 + Fe^{2+} \rightarrow ClO\cdot + Fe(OH)^{2+} \qquad (14)$$

$$ClO_2^- + Fe^{2+} + H_2O \rightarrow ClO\cdot + Fe(OH)_2^+ \qquad (15)$$

$$HClO_2 + ClO\cdot \rightarrow H^+ + ClO_3^- + Cl\cdot \qquad (16)$$

$$HClO_2 + Cl\cdot \rightarrow HOCl + ClO\cdot \qquad (17)$$

$$Cl\cdot + Fe^{2+} \rightarrow Cl^- + Fe^{3+} \qquad (18)$$

$$ClO\cdot + Fe^{2+} \rightarrow OCl^- + Fe^{3+} \qquad (19)$$

Supporting Equilibrium Reactions

$$Fe^{3+} + H_2O \leftrightarrows Fe(OH)^{2+} + H^+ \tag{20}$$

$$Fe^{3+} + 2H_2O \leftrightarrows Fe(OH)_2^+ + 2H^+ \tag{21}$$

$$Fe^{3+} + 3H_2O \leftrightarrows Fe(OH)_{3(s)} + 3H^+ \tag{22}$$

Total Chlorate Formation

The total amount of chlorate formation was predicted in simulations, where the parallel reactions were allowed to compete with each other. A simplified description of the competing chlorate formation paths is given in Scheme 1. Reactions assumed to contribute to Cl(III) consumption or affect the chlorate forming reactions in delignification environment (introduced below) were also incorporated. The reaction scheme used in total chlorate formation simulations included reactions (1), (5–26), and the autoprotolysis of water.

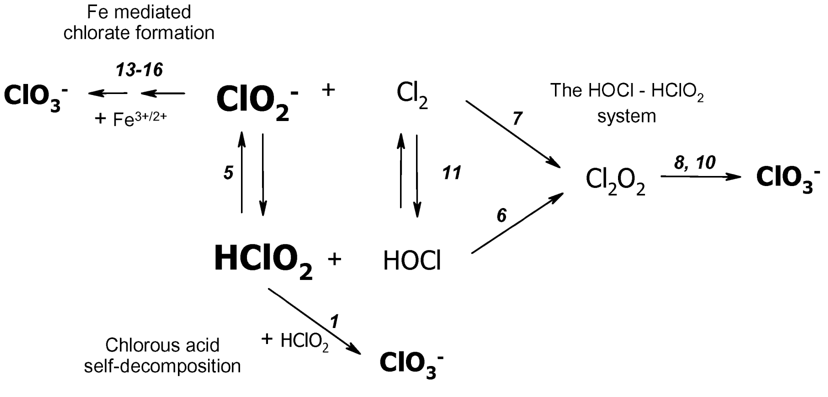

Scheme 1. A simplified description of the chlorate forming reaction paths (only the main reaction routes are shown).

Auxiliary Cl(III) Consuming Reactions

In a relatively acidic, chloride ion rich environment chlorous acid is consumed in reaction (23). The kinetic description and rate parameters ($k_{23} = 0.0027\,M^{-2}s^{-1}$ at 25°C, $E_{a,23} = 70$ kJ·mol^{-1}) were adopted from Lehtimaa et al.[35] Chlorous acid reacts at a moderate rate with aliphatic and aromatic aldehydes.[1,49,50] Reaction (24) represents these reactions. The aldehyde pseudo-compound

Org-CHO was assumed to be available in excess ([Org-CHO] = 10^{-2} M) and the rate coefficient was chosen to be in line with a value reported for chlorous acid oxidation of vanillin ($k_{24} = 1\ M^{-1}s^{-1}$, $k_{vanillin} = 2.1\ M^{-1}s^{-1}$ at 50°C).[50]

Auxiliary Reactions Affecting the Chlorate Formation Routes

Chlorous acid self-decomposition was assumed to perform unaffected in pulp suspensions (the same way as in aqueous solutions). The Cl and ClO radicals, in central role in Fe mediated Cl(III) decomposition, may react to some extent with pulp-related organic substrates. Experimental work has, however, shown that Fe additions in delignification promote chlorate yield considerably more than they promote AOX formation.[51] This supports the view that chlorite ion and chlorous acid are the primary substrates also in pulp suspensions. The hypochlorous acid concentration in delignification is very low at all times[39] due to fast reactions with chlorous acid and organic substrates. The low level of HOCl is likely to pose kinetic restrictions for overall reaction (2). Apparent overall reactions (25) and (26) represent the reactions of hypochlorous acid and elemental chlorine with pulp related organic substrates (lignin, hexenuronic acid, etc.). The organic substrate Org was available in excess ($[Org]_0 = 0.01$ M) and rate coefficients k_{25} and k_{26} were adjusted to values $k_{25} = 1 \cdot 10^6\ M^{-1}s^{-1}$ and $k_{26} = 2 \cdot 10^2\ M^{-1}s^{-1}$ at T = 50°C. The rate coefficient values, both the absolute magnitudes and the division of relative strength between Cl_2 (k_{25}) and HOCl (k_{26}), were chosen so that the combined reaction rate ($r_{25} + r_{26}$) was of the same order of magnitude as $r_{2,overall}$ ($= r_6 + r_7$) at pH 2 and declined toward a higher pH. The decline of ($r_{25} + r_{26}$) with pH was not as intensive as that of $r_{2,overall}$, which made the fraction of HOCl/Cl_2 consumed in organic reactions increase with pH. Consequently, the simulations showed a growing chlorite residue after pH 3.0. Similar observations concerning the chlorite residue have been observed also in delignification experiments.[4,13,17,19] If the combined reaction rate ($r_{25} + r_{26}$) was set higher, the chlorite residue appeared at a lower pH and vice versa. If the HOCl reaction (26) was appointed a higher relative strength, the pH dependence was more intense and the chlorite residue increased very drastically.

$$HClO_2 + Cl^- + H^+ \rightarrow 2HOCl \tag{23}$$

$$Org - CHO + HClO_2 \rightarrow Org - CO_2H + HOCl \tag{24}$$

$$Cl_2 + Org \rightarrow Org_{Cl} + H^+ + Cl^- \quad \text{(25—apparent overall reaction)}$$

$$HOCl + Org \rightarrow Org_{ox} + H^+ + Cl^- \quad \text{(26—apparent overall reaction)}$$

Initial Conditions

Typical delignification conditions (pH 1.5–4.0, 50°C, 60 min) were adopted from literature.[2,52] The pH range was investigated with 0.5 unit intervals. Inert buffer compounds were used to achieve and maintain the desired pH levels. The initial Cl(III) concentration was fixed based on mechanistic postulations concerning the reaction routes of chlorine dioxide in delignification.[1,4,5] The oxidation of the aromatic ring in lignin, either phenolic or non-phenolic, was assumed to proceed via a phenoxy radical (step 1) and yield quinonoid and muconic acid-type structures (step 2). The first step consumes one equivalent of ClO_2 and produces a full equivalent of Cl(III). The second step consumes another equivalent of ClO_2, and yields either Cl(III) or HOCl. Thus, the once through yield of Cl(III) is somewhere between 50 and 100%. Delignification experiments with intermediately formed hypochlorous acid trapped indicate that the overall HOCl yield is approximately 50–60%.[3,4,17,39] These values comprise hypochlorous acid from all sources: the HOCl arising directly from chlorine dioxide, but also that from chlorous acid self-decomposition or from reactions between chlorous acid and aldehydes. Based on this information it was assumed that step 2 produces mainly, but not entirely, hypochlorous acid and the one through yield of Cl(III) was set to be 67%. Assuming a 20 kg active chlorine/ ADt charge of ClO_2 and 10% pulp consistency, the 67% value corresponds to 8 mM concentration, which was used as the initial value for [Cl(III)] in all simulations.

Investigating the reaction between hypochlorous acid and chlorous acid requires specification of the initial hypochlorous acid and chloride ion concentration. Experimental studies have shown that the cumulative yield of hypochlorous acid is around 50% of the initial ClO_2 dose (pH 1.5–3.5).[4,17,39] The initial hypochlorous acid concentration was thus set to 6 mM. This setup does not give a completely authentic reproduction of the reaction conditions, because HOCl concentration in delignification is always at a low level (as explained in the previous section). The assumptions are nonetheless considered adequate for examining the overall reaction stoichiometry. Kinetic aspects of overall reaction (2) are evaluated in the section "Total Chlorate Production."

Chloride ion concentration is typically rather low in pulps entering ClO_2 delignification. A preceding hot acid stage using hydrochloric acid, or a suitable filtrate circulation arrangement, may result in a moderate chloride level. Thus a series of chloride concentrations (implemented as NaCl additions) were examined: $[Cl^-]_0 = 1, 2, 5,$ and 10 mM.

The iron content in Canadian kraft pulps is reported to be around 20–100 ppm.[53] Similar values have been measured from Finnish O-delignified birch kraft pulps.[54] We chose to use a low-end value, 20 ppm, as the dry pulp Fe content in the simulation. This value corresponds to approximately 0.02 mM in a 10% (consistency) pulp suspension. Iron is assumed to have a valence III (Fe^{3+}) in the initial state.

RESULTS AND DISCUSSION

In the first three sections the kinetic and stoichiometric restrictions of each individual chlorate-producing route are examined (in absence of all other reactions). In the last section the total amount and pH dependency of chlorate formation is predicted by making the routes compete with each other as well as with reactions assumed to affect Cl(III) consumption or chlorate formation in real delignification environment.

Chlorous Acid Self-Decomposition

Chlorous acid self-decomposition involves only one reactant and proceeds in a single step. Thus the stoichiometry is obvious (1) and the examination focuses on the reaction rate under typical delignification conditions. The simulated decomposition rates and the associated chlorate formation are shown in Figure 3. The chlorate curves at pH 3.5 and 4.0 coincide with the x-axis. The reaction rate is insignificant at pH 3.0 or above, reaches a notable level at pH 2.5 and increases steadily as the pH is further lowered. The pH dependence follows from the reaction being second order with respect to chlorous acid, and the protolysis equilibrium of $HClO_2$ (5) having a dissociation constant in the vicinity of 10^{-2} M (Table 1). Regardless of the accelerating effect of acidity, only about 70% of the Cl(III) has reacted in 1 hour at pH 1.5. Delignification experiments with end pH 2.1 and 1.8 (T = 50°C, 10% consistency) have shown that Cl(III) is fully consumed from the liquor in less than 30 and 15 minutes, respectively.[19]

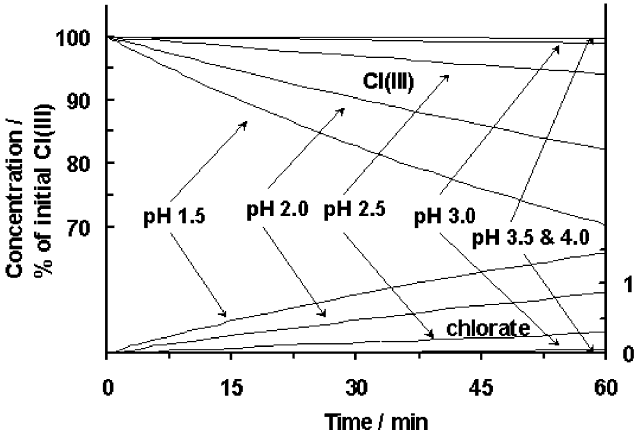

Figure 3. The effect of pH on chlorous acid self-decomposition rate and the related chlorate formation. T = 50°C, $[Cl(III)]_{initial}$ = 8 mM.

This means that chlorate production via chlorous acid self-decomposition is likely to be less than 10 percent of the available Cl(III) even at pH below 2.

The Reaction Between Chlorous Acid/Chlorite and Hypochlorous Acid/Chlorine

The simulated reactions were completed in a few seconds irrespective of the reaction conditions. The stoichiometric examinations were hence made from the final composition of the reaction solution. The final chlorine-containing products were chloride ion, chlorate ion, and hypochlorous acid. The hypochlorous acid residue is somewhat peculiar, but is explained by the absence of organic HOCl-consuming reactions (which are considered in a subsequent section). The intermediately produced chlorine dioxide was fully consumed in reaction (12). The product ratio (stoichiometry) depended on several factors: chloride ion concentration, Cl(III) concentration, and pH. The amount of chlorate in the final solution varied between 8 and 23% of the initial Cl(III) (Figure 4). Chlorate production was reduced both by increasing chloride ion concentration and pH. The effect of pH was, however, quite small after pH 2.5 (Figure 4). The effect of chloride ions was remarkably strong: raising the chloride ion concentration from 1 to 5 mM led to a roughly 30% reduction in chlorate formation.

The stoichiometric effects result from changes in the relative importance of parallel reactions (8–10), and to a minor extent from changes in equilibrium

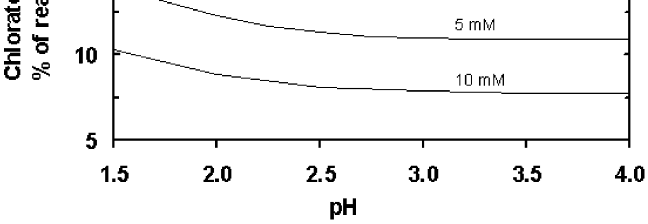

Figure 4. The effect of pH and chloride ion concentration on chlorate formation in the overall reaction of $HClO_2$ and HOCl. Results taken from the final composition in the solution (reactions completed). T = 50°C, $[Cl(III)]_{initial} = 8$ mM, $[HOCl]_{initial} = 6$ mM, reacted Cl(III) = initial Cl(III).

(11). The primary stoichiometric effect of chloride ions comes from the chloride ion catalysis in reactions (8) and (9). The rate of uncatalyzed reaction (8) is small and the magnitude of catalysis in that reaction is smaller than in reaction (9) (Table 2). Hence, chloride ions promote primarily the chlorine dioxide producing reaction (9) and a reduction in chlorate production is observed. As pH increases the protolysis equilibrium of chlorous acid (5) shifts toward chlorite ion. Reactions (9) and (10) have a first order rate dependence on chlorite ion and hence the increasing pH accelerates reactions (9) and (10) in comparison to the chlorate forming reaction (8). The effect of pH is very small above pH 3 because at this point Cl(III) is already almost entirely in the form of chlorite.

The yield of chlorate was also found to increase with a descending Cl(III) concentration. This might explain partially why the relative formation of chlorate is consistently higher in the brightening D stages than in delignification: ClO_2 charges, and hence also Cl(III) concentrations, are considerably smaller in the brightening stages than in delignification.[2,4,8,9,12,16,19,52,55]

Chlorate Formation Through Radical Chemistry

The rate of Fe mediated Cl(III) decomposition reduces with increasing pH already in the acidic region.[45,56] This results from the fact that Fe^{3+} forms various soluble and precipitated hydroxo species as well as polynuclear complexes.[45,56] The formation of aqueous and solid hydroxo-species was simulated to elucidate the effect of pH (Table 4). Indeed, the fraction of the hydroxo-species increases dramatically with pH. At pH 3 almost all Fe^{3+} has precipitated.

The rate of Fe mediated Cl(III) decomposition and the related chlorate formation are shown in Figure 5. The effect of pH is dramatic: the rate is insignificant at pH 3.5 and 4.0 and still very slow at pH 3.0, but already at pH 2.5 more than 95% of the initial Cl(III) has reacted in 60 minutes. The rate exhibits a maximum between pH 1.5–2.0. In the heavily acidic region

Table 4. The hydroxylation of Fe^{3+} at pH = 1.5–4.0. T = 50°C, $[Fe(III)]_{tot} = 20\ \mu M$

	Fe(III) distribution/%		
pH	Fe^{3+}	$Fe(OH)^{2+}$ and $Fe(OH)_2^+$	$Fe(OH)_3(s)$
1.5	56	44	—
2.0	29	71	—
2.5	3	24	73
3.0	0.1	0.9	99
3.5	<0.1	<0.1	100
4.0	<0.1	<0.1	100

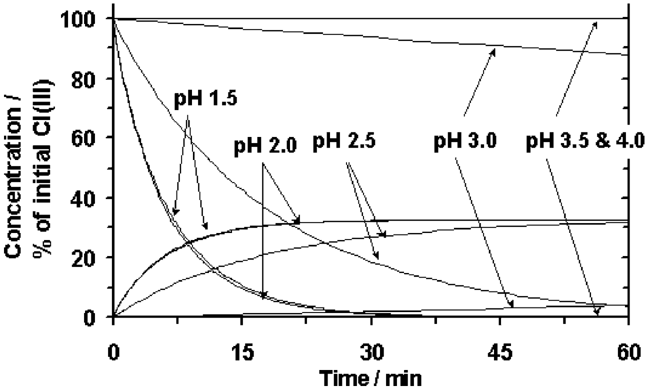

Figure 5. The effect of pH on Fe mediated Cl(III) decomposition and the related chlorate formation. Curves starting from 0% represent chlorate concentrations and those starting from 100% represent Cl(III) concentrations. T = 50°C, $[Cl(III)]_{initial} = 8$ mM, $[Fe]_{tot} = 20\ \mu M$.

(pH < 1.5) the rate declines again as chlorite protonation increases (reaction 5) and slows down the reaction (13_{for}). The rate hindrance due to chlorite protonation is counterbalanced by an increasing fraction of *free* Fe^{3+} ions (Table 4), but the net effect is still suppressing. The rate decrease above pH 2 follows directly from Fe^{3+} hydroxylation (Table 4). Chlorate production is negligible above pH 3, but at pH 2.5 or below the yield is around 25–35% of available Cl(III). The other stable chlorine-containing products, hypochlorous acid and chloride ion, were produced in approximately 1:1 ratio irrespective of the pH.

Total Chlorate Production in Delignification

Some 10–18% of the initial chlorine dioxide dose is typically converted to chlorate in ClO_2 delignification at pH 1.5–2.5.[4,16,19,55] The chlorate yield reduces after pH 2.5 and is a few percent at neutral pH.[13,17,19] The rather broad range of experimental findings at a fixed pH shows that chlorate formation is a function of also other variables (for instance, pulp consistency, temperature). The predicted chlorate formation is compared against experimental findings in Figure 6. The prediction falls into the range of experimental findings. The pH dependence is also in accordance. The coherence of the estimate implies that radical generation through two-electron reduction of chlorine dioxide, excluded from the model, is likely to have only a small importance.

The individual reaction route simulations suggest that the rate of chlorous acid self-decomposition is too slow to compete against Fe mediated Cl(III)

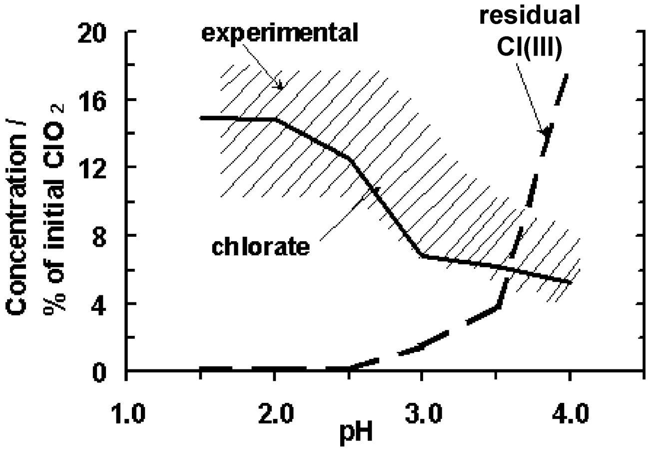

Figure 6. Total chlorate production as a function of pH. The diagonal bars indicate the range of experimentally observed chlorate formation.[4,16,19,55] Simulation conditions: reaction time = 45 min, T = 50°C, $[Cl(III)]_{initial} = 8$ mM, $[Cl^-]_{initial} = 1$ mM.

decomposition at any investigated pH (Figures 3 and 5). The importance of the first route is hence expected to be small. This was confirmed by excluding chlorous acid self-decomposition from one set of simulations. The difference to the original simulation was insignificant (less than 1 percent). Hence, at pH below 3 chlorate formation results entirely from Fe mediated Cl(III) decomposition and overall reaction (2). At pH ≥ 3 only the latter route produces chlorate (Figure 5). The simulations showed an increasing chlorite residue at pH 3 or above (Figure 6).

It was also observed that reaction (23) had no practical importance. Excluding the reaction from the simulation changed the final concentrations less than 0.1%. The effect was insignificant, even if the chloride ion concentration was increased to 10 mM. The half-life of the reaction (at constant $[Cl^-] = 10$ mM and pH 1.5, T = 50°C) is approximately 31 hours. Obviously, reaction (23) requires a much higher acidity, temperature, and/or a higher chloride ion concentration to have importance.

The somewhat low total chlorate yield prediction at pH 3–4 may result from the fact that, despite the acidic conditions in the final solution, the neutral or mildly alkaline pulp entering delignification may still provide favorable conditions for alkaline chlorine dioxide decomposition (4) at the very beginning of the process.

The simulation examples and their coherence with experimental findings bring forth several advantages of the used approach. The execution of simulations is not limited by existing laboratory, pilot scale, or mill equipment. Laboratory experiments typically suffer from limitations in the number of experiments, sampling points, or analyzed components. Simulative examinations are not oppressed by such constraints. The reaction routes and role of fast-lived intermediates, whose concentrations are usually below the detection limit of experimental methods, are brought accessible for investigation. Simulations may also be used to guide and reduce the amount of experimental work done in laboratory. The fundamentality of the approach enables simulations to be extended outside the condition range in which the kinetic parameters are determined. In future work the model may be augmented with comprehensive descriptions of chlorine dioxide, hypochlorous acid, and chlorine-consuming organic reactions. If successful, this would provide completely new possibilities to assess and optimize the delignification process with respect to chemical dosing, AOX formation, and chlorate formation.

CONCLUSIONS

Fe mediated Cl(III) decomposition and the reaction between hypochlorous acid and chlorous acid (or their equilibrium counterparts) are the major reaction routes responsible for chlorate formation in ClO_2 delignification. Both reactions contain steps that facilitate chlorine dioxide reformation, and complete blocking of the overall reactions is not advisable. Process variable adjustments may, however, be used to manage chlorate formation. Fe mediated Cl(III) decomposition yields chlorine dioxide in a ratio inferior to the reaction between hypochlorous acid and chlorous acid. Thus, chlorine dioxide reformation via the latter reaction should be favored. This is achieved by maintaining the delignification end pH around 3–3.5. The pH should not be increased over 3.5 due to an increasing chlorite residue. The stoichiometry of the reaction between hypochlorous acid and chlorous acid may be directed toward low chlorate yield by ensuring a moderate chloride ion concentration. High consistencies are also to be favored due to the fact that dilute conditions promote chlorate formation. This study demonstrates, in general, the opportunities of kinetic modeling: the behavior of complex reaction systems may be examined in a fast and economic manner.

NOMENCLATURE

A	frequency factor (reaction dependent)
E_a	activation energy ($J \cdot mol^{-1}$)
G_f	Gibb's energy of formation ($J \cdot mol^{-1}$)
H_f°	heat of formation ($J \cdot mol^{-1}$)
K	equilibrium constant (reaction dependent)
k	rate constant (reaction dependent)
R	gas constant (8.3144 $J \cdot K^{-1} \cdot mol^{-1}$)

S°	entropy ($J \cdot K^{-1} \cdot mol^{-1}$)
T	temperature (K)

ABBREVIATIONS

[A]	concentration of species A (M)
ADt	air dry ton of pulp
AOX	adsorbable organic halogens
M	mol/dm^3

REFERENCES

1. Lindgren, B.O. Chlorine dioxide and chlorite oxidations of phenols related to lignin. Svensk papperstidn. **1971**, *74*(3), 57–63.
2. Dence, C.W.; Reeve, D.W. *Pulp Bleaching: Principles and Practice*; Tappi Press: Atlanta, GA, United States, 1996.
3. Ni, Y.; Shen, X.H.; Van Heiningen, A.R.P. Studies on the reactions of phenolic and nonphenolic lignin model compounds with chlorine dioxide. J. Wood Chem. Technol. **1994**, *14*(2), 243–262.
4. Kolar, J.J.; Lindgren, B.O.; Pettersson, B. Chemical reactions in chlorine dioxide stages of pulp bleaching: Intermediately formed hypochlorous acid. Wood Sci. Technol. **1983**, *17*(2), 117–128.
5. Brage, C.; Eriksson, T.; Gierer, J. Reactions of chlorine dioxide with lignins in unbleached pulps. Part I. Reactions of chlorine dioxide with monomeric model compounds representing aromatic structures in residual lignins. Holzforschung **1991**, *45*(1), 23–30.
6. Fredricks, P.S.; Lindgren, B.O.; Theander, O. Chlorine oxidation of cellulose. IV. Kinetics and mechanisms of the reactions of methyl b-D-glucopyranoside with chlorine in acid aqueous solution. Svensk papperstidn. **1971**, *74*(19), 597–603.
7. Marpillero, P. The bleaching of pulps with activated chlorate. Tappi **1958**, *41* (5), 213A–216A.
8. Rapson, W.H.; Anderson, C.B. Improving the efficiency of chlorine dioxide bleaching. Transactions Tech. Sect. CPPA **1977**, *3*(2), TR52–TR55.
9. Bergnor, E.; Germgard, U.; Kolar, J.J.; Lindgren, B.O. Formation of chlorate in chlorine dioxide bleaching. Cellulose Chem. Technol. **1987**, *21*(3), 307–314.
10. van Wijk, D.J.; Hutchinson, T.H. The ecotoxicity of chlorate to aquatic organisms: A critical review. Ecotoxicol. Environ. Safety **1995**, *32*(3), 244–253.
11. Lindgren, B.O.; Nilsson, T. Chlorate formation during reaction of chlorine dioxide with lignin model compounds. Svensk Papperstidn. **1975**, *78*(2), 66–68.
12. Nilsson, T.; Sjostrom, L. Losses in chlorine dioxide as a result of chlorate formation during bleaching. Svensk Papperstidn. **1974**, *77*(17), 643–647.
13. Rapson, W.H.; Anderson, C.B. Kraft Pulp bleaching with chlorine and chlorine dioxide—Effect of pH on the chlorination stage. Tappi J. **1978**, *61*(10), 97–99.

14. Soila, R.; Lehtikoski, O.; Virkola, N.-E. On the reactions taking place during the chlorine dioxide bleaching stage. Svensk Papperstidn. **1962**, *65*(12), 632–638.
15. Germgard, U.; Teder, A.; Tormund, D. Chlorate formation during chlorine dioxide bleaching of softwood kraft pulp. Paperi Puu **1981**, *63*(3), 127–133.
16. Ni, Y.; Kubes, G.J.; Van Heiningen, A.R.P. Mechanism of chlorate formation during bleaching of kraft pulp with chlorine dioxide. J. Pulp Paper Sci. **1993**, *19*(1), J1–J6.
17. Yoon, B.; Wang, L.; Yoon, S.; Kim, S. Mechanism of chlorate formation in chlorine dioxide delignification. Appita J. **2004**, *57*(6), 472–474.
18. Svenson, D.R.; Kadla, J.F.; Chang, H.; Jameel, H. Effect of pH on the inorganic species involved in a chlorine dioxide reaction system. Ind. Eng. Chem. Res. **2002**, *41*(24), 5927–5933.
19. Svenson, D.R.; Jameel, H.; Chang, H.; Kadla, J.F. Inorganic reactions in chlorine dioxide bleaching of softwood kraft pulp. J. Wood Chem. Technol. **2006**, *26*(3), 201–213.
20. Yoon, B.-H.; Wang, L.-J. Chlorate reduction in ClO_2 prebleaching by the addition of hypochlorous acid scavengers. J. Pulp Paper Sci. **2002**, *28*, 274–279.
21. Kolar, J.J.; Lindgren, B.O. Oxidation of styrene by chlorine dioxide and by chlorite in aqueous solutions. Acta Chem. Scand. **1982,** *36* B(9), 599–605.
22. Wartiovaara, I. Theoretical model for reaction mechanism of chlorine dioxide bleaching. Paperi ja Puu **1982**, *64*(11), 680–683.
23. Gordon, G.; Kieffer, R.G.; Rosenblatt, D.H. The chemistry of chlorine dioxide. Prog. Inorg. Chem. **1972**, *15*, 201–286.
24. Von, H.G.; Teder, A. Kinetics of the decomposition of aqueous chlorine dioxide solutions. Acta Chem. Scand. **1973**, *27*(10), 4018–4019.
25. Wartiovaara, I. The influence of pH on the D stages of DE and ODE bleaching sequences. Paperi ja Puu **1982**, *64*(10), 581–584.
26. Taube, H.; Dodgen, H. Applications of radioactive chlorine to the study of the mechanisms of reactions involving changes in the oxidation state of chlorine. J. Am. Chem. Soc. **1949**, *71*, 3330–3336.
27. Hong, C.C.; Rapson, W.H. Kinetics of disproportionation of chlorous acid. Can. J. Chem. **1968**, *46*(12), 2053–2060.
28. Fabian, I.; Gordon, G. Iron(III)-catalyzed decomposition of the chlorite ion: An inorganic application of the quenched stopped-flow method. Inorg. Chem. **1992**, *31*(11), 2144–2150.
29. Horvath, A.K.; Nagypal, I.; Peintler, G.; Epstein, I.R.; Kustin, K. Kinetics and mechanism of the decomposition of chlorous acid. J. Phys. Chem. A **2003**, *107*(36), 6966–6973.
30. Peintler, G.; Nagypal, I.; Epstein, I.R. Systematic design of chemical oscillators. 60. Kinetics and mechanism of the reaction between chlorite ion and hypochlorous acid. J. Phys. Chem. **1990**, *94*(7), 2954–2958.
31. Schmitz, G.; Rooze, H. Reaction mechanisms for chlorite and chlorine dioxide. 1. Stoichiometry of chlorite reactions and kinetics in the presence of ortho-toluidine. Can. J. Chem. **1981**, *59*(8), 1177–1187.
32. Jakobsson, K.; Aittamaa, J. Introduction to Flowbat software; http://www.tkk.fi/Units/ChemEng/research/Software/flowbat/index.html (accessed September 2008).

33. Kieffer, R.G.; Gordon, G. Disproportionation of chlorous acid. I. Stoichiometry. Inorg. Chem. **1968**, *7*(2), 235–239.
34. Emmenegger, F.; Gordon, G. The rapid interaction between sodium chlorite and dissolved chlorine. Inorg. Chem. **1967**, *6*(3), 633–635.
35. Lehtimaa, T.; Tarvo, V.; Mortha, G.; Kuitunen, S.; Vuorinen, T. The reactions and kinetics of Cl(III) decomposition. Ind. Eng. Chem. Res. **2008**, *47*(15), 5284–5290.
36. Dean, J.A. *Lange's Handbook of Chemistry;* McGraw-Hill Inc.: New York, USA, 1999.
37. Aieta, E.M.; Roberts, P.V. Kinetics of the reaction between molecular chlorine and chlorite in aqueous solution. Environ. Sci. Technol. **1986**, *20*(1), 50–55.
38. Connick, R.E.; Chia, Y. The hydrolysis of chlorine and its variation with temperature. J. Am. Chem. Soc. **1959**, *81*, 1280–1284.
39. Ni, Y.; Kubes, G.J.; Van Heiningen, A.R.P. Rate processes of chlorine species distribution during chlorine dioxide prebleaching of kraft pulp. Nord. Pulp Paper Res. J. **1992**, *7*(4), 200–204.
40. Wang, T.X.; Margerum, D.W. Kinetics of reversible chlorine hydrolysis: Temperature dependence and general-acid/Base-assisted mechanisms. Inorg. Chem. **1994**, *33*(6), 1050–1055.
41. Rapson, W.H.; Anderson, C.B. Mixtures of chlorine dioxide and chlorine in the chlorination stage of pulp bleaching. Pulp & Paper Magazine of Canada **1966**, *67*(1), T47–T55.
42. Ondrus, M.G.; Gordon, G. Oxidation of hexaaquoiron(II) by chlorine(III) in aqueous solution. Inorg. Chem. **1972**, *11*(5), 985–989.
43. Schmitz, G.; Rooze, H. Reaction mechanism for chlorite and chlorine dioxide. 3. Disproportionation of chlorite. Can. J. Chem. **1985**, *63*(4), 975–980.
44. Schmitz, G.; Rooze, H. Reaction mechanism for chlorite and chlorate. 2. Reaction kinetics of chlorite in the presence of o-Tolidine. Can. J. Chem. **1984**, *62*(11), 2231–2234.
45. Fabian, I.; Gordon, G. Kinetics and mechanism of the complex formation of the chlorite ion and iron(III) in aqueous solution. Inorg. Chem. **1991**, *30*(21), 3994–3999.
46. Jakobsson, K.; Aittamaa, J., *KINFIT User's Manual*; http://www.tkk.fi/Units/ChemEng/research/Software/kinfit/KINFIT_eng.html (accessed September 2005).
47. Kormanyos, B.; Horvath, A.K.; Peintler, G.; Nagypal, I. Inherent pitfalls in the simplified evaluation of kinetic curves. J. Phys. Chem. A **2007**, *111*(33), 8104–8109.
48. Press, W.H.; Flannery, B.P.; Teukolsky, S.A. *Numerical Recipes—The Art of Scientific Computing (FORTRAN Version);* Cambridge University Press: Cambridge, 1989.
49. Jeanes, A.; Isbell, H.S. Chemical reactions of the chlorites with carbohydrates. J. Research Natl. Bur. Standards **1941**, *27*, 125–142 (Research Paper No. 1408).
50. Lehtimaa, T., Tarvo, V., Mortha, G., Vuorinen, T., The role of chlorite in chlorine dioxide bleaching, *Proceedings from the 14th ISWFPC*; TAPPSA: Durban, SA, 2007.
51. Joncourt, M.J.; Froment, P.; Lachenal, D. Formation of radical species during ClO_2 delignification. J. Wood Chem. Technol. **1998**, *18*(2), 159–170.

52. Fogelholm, C.J. *Papermaking Science and Technology 6A. Chemical Pulping*; Fapet Oy: Jyväskylä, 2000.
53. Lapierre, L.; Bouchard, J.; Berry, R.M.; Van Lierop, B. Chelation prior to hydrogen peroxide bleaching of kraft pulps: Overview. J. Pulp Paper Sci. **1995**, *21*(8), 268–273.
54. Räsänen, E.; Kärkkäinen, L. Modelling of complexation of metal ions in pulp suspensions. J. Pulp Paper Sci. **2003**, *29*(6), 196–203.
55. Medina, J., Lehtimaa, T., Tervola, P., Vehmaa, J., Pikka, O., Vuorinen, T., Chlorate reduction in Eucalyptus pulp bleaching, *Conference Proceedings, IPBC 2008*; PAPTAC: Montreal, QC, Canada, 229–231.
56. Fabian, I.; Gordon, G. Complex formation reactions of the chlorite ion. Inorg. Chem. **1991**, *30*(19), 3785–3787.